A window radiation chart for estimating surface temperature from satellite observations

By OLOV LÖNNQVIST, *The Swedish Meteorological and Hydrological Institute, Stockholm*

(Manuscript received November 6, 1962; revised version October 19, 1963)

ABSTRACT

A special radiation chart is constructed for estimating surface temperature from the outgoing terrestrial radiation in the window region. Estimates obtained are compared with recently published numerical estimates.

1. Introduction

Measurements of the outgoing radiation in the so-called "water-vapor window" have been carried out from meteorological satellites in order to obtain estimates of the temperature of the underlying surface. Comparisons made by FRITZ & WINSTON (1962), NORDBERG, BANDEEN, CONRATH, KUNDE & PERSANO (1962) and others, show that in practically all cases the effective temperature in the window region is lower than the surface temperature. A radiation diagram specially designed for this purpose would be a convenient tool for clearly demonstrating this fact. It could be used for determining standard corrections to be applied under various atmospheric conditions. In addition, such a diagram could possibly be utilized as a routine device on receipt of satellite data at places where electronic computers are not available for the interpretation of radiation observations.

2. Radiation charts for the total terrestrial radiation

ELSASSER (1942), MÖLLER (1943), ROBINSON (1950) & YAMAMOTO (1952) have constructed well-known radiation charts. These charts and others constructed for the same purpose have been compared by the present author (1954), KONDRATIEV & NIILISK (1960) and others. The comparisons show that the diagrams differ not only in their construction but also as to the numerical results they give. The differences in construction can easily be overcome. In full agreement with YAMAMOTO (1952), the author has found the Kew radiation chart, proposed by ROBINSON, to be the most convenient. It is reproduced in the upper part of Fig. 1. In the lower part we have for comparison the Elsasser chart, here transformed from its well-known triangular shape into the same rectangular form as the Kew chart.

YAMAMOTO (1952) has discussed in detail the background to the different way of drawing the isopleths for the optical depth u' in the two charts. The curvature of the isopleths in the Elsasser chart is justifiable theoretically. In the Kew chart, which is an empirical diagram, the isopleths were intentionally drawn in a very simple way.

In Fig. 1 we have plotted the u'–T relationship according to the ICAO Standard Atmosphere, assuming 60 per cent relative humidity at all levels. Plotted data are shown by a broken line in both charts. The optical depth is counted downwards from the top of the atmosphere. In correcting the optical depth for pressure broadening of the spectral lines, we have used the square root law. The same law has been used elsewhere in this paper.

In both charts the area to the right of the broken line corresponds to the total upward radiation flux at the top of the atmosphere. The dotted line is drawn in such a way that the area to its right is equal to the area to the right of the broken line. Obviously, the dotted line indicates the effective temperature of the earth–atmosphere system as observed from above

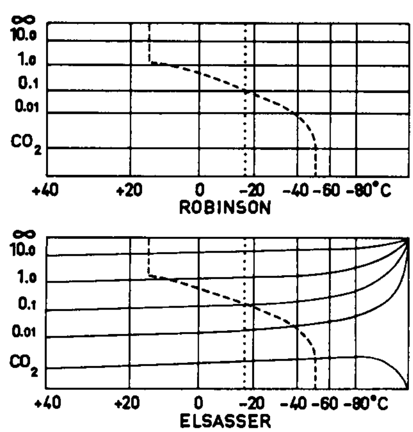

FIG. 1. Radiation charts for the total radiation; Kew chart above, Elsasser chart below. The latter has been transformed into rectangular form. Broken line shows a certain temperature–humidity distribution. The area to the right of the broken line represents upward flux at the top of the atmosphere. Dotted line indicates effective temperature.

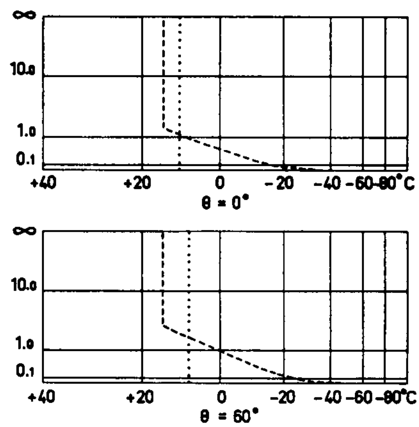

FIG. 2. Window radiation chart (8.7–11.8 μ). Broken line represents the same atmosphere as in Fig. 1. In the upper chart the beam is vertical, in the lower one the nadir angle $\theta = 60°$. Dotted lines show effective temperatures in the window region.

within the total range of terrestrial radiation. In both cases the effective temperature is found to be equal to $-17°C$.

3. A radiation chart for the window region of the infrared water-vapor spectrum

If the window is defined as the most transparent part of the infrared spectrum of water vapor, it is convenient to specify its limits as 8.7 and 11.8 microns (1150 and 850 cm^{-1}, respectively). A radiation chart for the window so defined is reproduced twice in Fig. 2. The vertical axis carries a scale for $u'/\cos\theta$, i.e. the optical depth in g/cm^2, corrected for pressure broadening, and divided by $\cos\theta$, where θ is the nadir angle. The horizontal axis carries a temperature scale. The chart is based on values for the average transmissivity for a column, $\tau_l\{u(T)\}$, and the generalized absorption coefficient, l_ν, given by YAMAMOTO (1952).

The same u'–T relationship already used in Fig. 1 is plotted in the two charts of Fig. 2. In the upper chart the nadir angle is equal to zero, in the bottom one it is equal to 60 degrees. The figure demonstrates the extent to which the nadir angle affects the effective temperature in the window region. In the case studied the surface temperature is $+15°C$, the effective temperature is $+11°C$ for a vertical beam and $+8°C$ for the oblique beam.

So far we have disregarded the presence of a strong ozone band at about 9.6 μ. In constructing the radiation chart it would have been possible to account for the effect of ozone in a similar way to that in which the carbon-dioxide effect has been accounted for in radiation charts for the total radiation (see Fig. 1). A quite different method that seems more convenient will be discussed in section 4.

It should be mentioned here that GREENFIELD & KELLOGG (1960) used a diagram rather like the one discussed above, though they did not use it for the same purpose. After presenting the original version of this paper the author has become aware of a similar attempt by MÖLLER (1962).

The radiation chart shown in Fig. 2 should not be used for interpreting radiation measurements in TIROS channel 2. According to the TIROS II manual, published by NASA (1961*b*), channel 2 extends from 7.5 to 13.5 microns, and the effective spectral response varies considerably within that region. Using the response as a weighting function, it is possible to obtain a special radiation chart for TIROS channel 2. This is reproduced in Fig. 3. The horizontal axis carries a temperature scale corresponding to the effective black-body radiation in channel 2. The flux in w/m^2 is given parallel with the temperature scale.

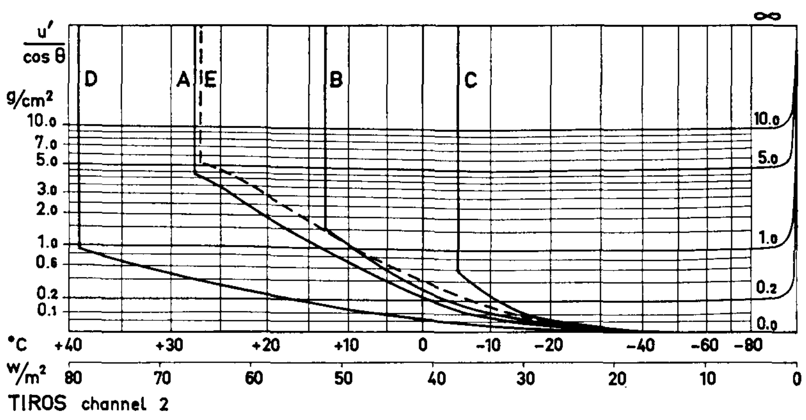

FIG. 3. The TIROS channel 2 radiation chart. Curves drawn represent the following type atmospheres: A, B and C average conditions in March in the latitude belts 0°–10° N, 30°–40° N and 50°–60° N, respectively; D over a desert; E an extremely moist atmosphere. Nadir angle equal to zero.

4. Ozone correction

According to a numerical investigation by WARK, YAMAMOTO & LIENESCH (1962), published after the first version of this paper had been completed, a good approximation of the outgoing radiation can be obtained by first computing the outgoing radiation from an ozone-free atmosphere and then applying an ozone correction. They found that the same correction applies to any zenith (or nadir) angle. From Fig. 7*a* (loc. cit.) we have computed correction figures in degrees Celsius, and these are given in Table 1.

5. Surface temperature evaluations for various type atmospheres

The radiation chart of Fig. 3 contains curves for five type atmospheres. Curves A, B and C represent atmospheres discussed by LONDON (1952). They show average conditions during March in the latitude belts 0°–10° N, 30°–40° N and 50°–60° N, respectively. Type atmosphere D has been chosen to characterize the atmosphere over a desert. Data were taken from Colomb-Béchar, Sahara, on 15 July 1961, i.e. the day for TIROS III observations over Egypt, discussed by NORDBERG *et al.* (1962). Type E, finally, is an example of an extremely

TABLE 1. *Ozone corrections.*

To obtain the true effective temperature, subtract the appropriate figure in the table from the effective temperature read from the TIROS channel 2 radiation chart.

Effective temperature (read from Chart)								
+40	+30	+20	+10	±0	−10	−20	−30	°C
Ozone correction								
3.9	3.7	3.4	3.1	2.8	2.5	2.1	1.7	

TABLE 2. *Differences between surface temperature and effective temperature.*

Type atmosphere	Height of radiating surface (km)	Temperature at radiating surface (°C)	Difference between surface temperature and effective temperature (°C) $\theta = 0°$	$\theta = 60°$
A	0	+27.7	11.6	15.0
(0°–10° N)	1	+22.8	9.6	12.4
	2	+18.2	7.8	10.3
	4	+7.8	5.2	6.4
B	0	+13.0	7.2	9.3
(30°–40° N)	1	+9.0	6.0	7.8
	2	+4.4	5.1	6.6
	4	−6.3	3.5	4.1
C	0	−5.0	4.3	5.5
(50°–60° N)	1	−8.5	3.7	4.7
	2	−11.9	3.2	4.0
	4	−21.5	2.4	2.9
D	0	+39	8.8	11.3
(desert)	1	+26	5.9	7.5
	2	+16	4.6	5.6
	4	0	3.2	3.6
E	0	+27	13.3	17.5
(extremely	1	+21	10.8	14.1
high	2	+15	8.4	11.1
humidity)	4	+4	5.3	6.9

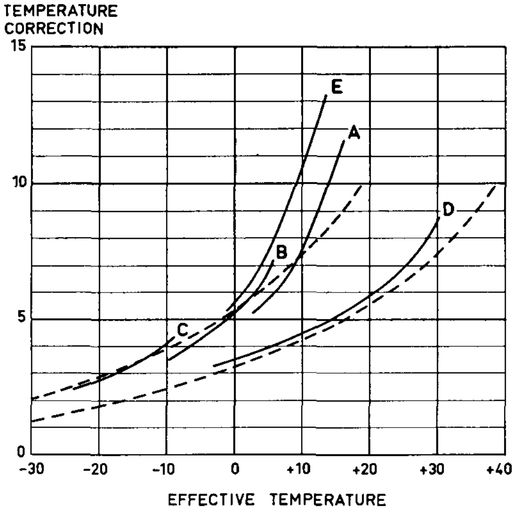

FIG. 4. Correction terms (in degrees Celsius) to be added to the effective temperature observed in TIROS channel 2 in order to obtain the surface temperature. Nadir angle is equal to zero. Full curves represent type atmospheres given in Fig. 3. Broken curves are taken from WARK *et al.* They indicate corrections for typical high (upper curve) and low (lower curve) humidity cases.

moist atmosphere. Data were taken from Albrook, Panama, on 15 September 1961.

For each one of the five type atmospheres presented in Fig. 3 we have evaluated the difference between the surface temperature and the effective temperature which would have been observed in TIROS channel 2. Similar evaluations have been carried out for cloud-top surfaces assumed to be located at 1, 2 and 4 km above the surface of the earth. In each case the original temperature–humidity distribution has been used in the layer above the cloud tops. The results are given in Table 2. All values are corrected for ozone in accordance with Table 1.

The results given in Table 2 are presented in a different and more appropriate way in Fig. 4. From the curves in the figure we find for each value of the effective temperature observed from the satellite an indication of the magnitude of the correction term which should be added to the effective temperature in order to obtain the true surface temperature. Full lines indicate corrections found by the graphical method discussed in this paper. Broken lines show corrections found by the numerical method recently presented by WARK *et al.* (1962). The upper broken curve represents typical high humidity cases, the lower one represents low humidity cases.

The corrections shown in Fig. 4 are applicable when the radiometer is directed vertically. For a nadir angle equal to 60 degrees the corrections should be multiplied by a factor which varies between 1.2 and 1.8 depending on the type of atmosphere.

Fig. 4 indicates the necessity of making a reasonable assumption as to the actual temperature–humidity distribution in the atmosphere in order to obtain from TIROS channel 2 observations a reliable estimate of the surface temperature. We also need the nadir angle, for which reason data tabulations like the one already published by NASA (1961*a*) should preferably indicate the nadir angle for each part of the radiation maps.

It is easily seen by plotting appropriate data in the window radiation chart that inversions immediately above the surface reduce the difference between the surface temperature and the effective temperature. Under extreme conditions the difference could even have a negative value.

To test the estimation method, corrections found in Fig. 4 were applied to the observations discussed by NORDBERG *et al.* (1962). Over the Egyptian desert TIROS III indicated a temperature of about +35°C. From Fig. 4 the most likely correction would be 9°. This would imply a surface temperature of about +44°C, which might be correct. At the actual time temperatures at screen level were about +39°C in the area. Over the Atlantic Ocean off the northeast coast of Brazil and over Lake Michigan, however, the temperatures observed from the satellite over clear sky areas are much too low even when corrected for the water-vapor and ozone effect. One possible explanation apart from instrumental errors might be a certain contribution to the effective radiation emanating from tops of surrounding clouds or some scattered clouds in the area.

REFERENCES

ELSASSER, W. M., 1942, Heat transfer by infrared radiation in the atmosphere. *Harvard Met. Studies*, **6**, pp. 107.

FRITZ, S., and WINSTON, J. S., 1962, Synoptic use of radiation measurements from satellite TIROS II. *Monthly Weather Rev.*, **90**, pp. 1–9.

GREENFIELD, S. M., and KELLOGG, W. W., 1960, Calculations of atmospheric infrared radiation as seen from a meteorological satellite. *J. of Met.*, **17**, pp. 283–290.

KONDRATIEV, K. Y., and NIILISK, H. I., 1960, Comparison of radiation charts. *Geofisica Pura e Applicata*, **46**, pp. 231–240.

LONDON, J., 1952, The distribution of radiational temperature change in the Northern Hemisphere during March. *Geophys. Research Papers*, 18, 64 pp.

LÖNNQVIST, O., 1954. Synthetic formulae for estimating effective radition to a cloudless sky and their usefulness in comparing various estimation procedures. *Arkiv Geofys.*, **2**, pp. 245–294.

MÖLLER, F., 1943, *Das Strahlungsdiagramm*. Berlin, Springer-Verlag, 13 pp.

MÖLLER, F., 1962, Einige vorläufige Auswertungen der Strahlungsmessungen von TIROS II. *Arch. Met. Geophys. u. Bioklim.*, Serie B, **12**, pp. 78–94.

NASA Goddard Space Flight Center, 1961*a*, *TIROS II Radiation Data Catalog*. 356 pp.

NASA Goddard Space Flight Center, 1961*b*, *TIROS II Radiation Data User's Manual*. 54 pp.

NORDBERG, W., BANDEEN, W. R., CONRATH, B. J., KUNDE, V., and PERSANO, I., 1962, Preliminary results of radiation measurements from the TIROS III meteorological satellite. *J. of Atm. Sciences*, **19**, pp. 20–30.

ROBINSON, G. D., 1950, Notes on the measurement and estimation of atmospheric radiation—2. *Quart. J. Roy. Met. Soc.*, **76**, pp. 37–51.

WARK, D. Q., YAMAMOTO, G., and LIENESCH, J. H., 1962, Methods of estimating infrared flux and surface temperature from meteorological satellites. *J. of Atm. Sciences*, **19**, pp. 369–384.

YAMAMOTO, G., 1952, On a radiation chart. *Science Rep. Tôhoku Univ. (Sendai), Geophys.*, **4**, pp. 9–23.